Restriction of HSV-1 replication by pistachios (Pistacia vera L.) reveals a promising strategy for regulating virus-mediate chemokine response in THP-1 cells

Rosamaria Pennisi
University of Messina
Marianna Costa
University of Messina
Maria Pia Tamburello
University of Messina
Paola Trischitta
University of Messina
Giuseppina Mandalari
University of Messina
Maria Teresa Sciortino
mtsciortino@unime.it
University of Messina

Article

Keywords: HSV-1, Pistacia vera extracts, NF-κB signaling, Chemokines, Antiviral activity, Inflammation

Posted Date: September 5th, 2025

DOI: https://doi.org/10.21203/rs.3.rs-7244476/v1

Additional Declarations: No competing interests reported.

Version of Record: A version of this preprint was published at Scientific Reports on March 28th, 2026.
See the published version at https://doi.org/10.1038/s41598-026-43975-x.

Abstract

In recent years, great interest has been committed to the search for alternative clinical treatments for herpetic infections that reduce side effects, overcome drug resistance phenomena, and fight the intense inflammatory response triggered by viral infection. Polyphenols are well-known pharmacologically active compounds with both immunomodulatory and antiviral activity present in large quantities in pistachios (*Pistacia vera L.*). The present work investigates the antiviral properties of pistachio extracts against HSV-1 and their potential immunomodulatory effect on human monocytic cells, with a focus on NF-κB signaling. RT^2 profiler PCR array was used to identify differential gene expression levels of chemokines during infection and pretreatment. We discovered that HSV-1 induces a potent activation of cytokines and chemokines in monocytes entirely abrogated by *in vitro* treatment with pistachio extracts. Our focus included the CXCL10, CXCL11, CCL13, CCL2, CCL4, CCL13 and the receptor CMKLR1, particularly expressed following HSV-1 replication and downregulated upon pistachio extracts pretreatment, we further confirmed this inhibitory activity using zeaxanthin, a bioactive carotenoid found in pistachios, previously shown to inhibit HSV-1 replication in permissive cells. In addition, by blocking viral replication with phosphonoacetic acid, we demonstrated that in HSV-1-infected THP-1 cells, the activation of CXCL10, CXCL11, CCL13, CCL2, CCL4, CCL13 and the receptor CMKLR1, was wholly abrogated, suggesting that chemokine activation is strictly dependent on active HSV-1 replication. Lastly, using THP-1-dnIκBα cells, we have demonstrated that chemokine accumulation was correlated with HSV-1-induced NF-κB activation. This study highlights the use of pistachio extracts and zeaxanthin as a promising therapeutic approach against HSV-1. Notably, it offers valuable insights into the complex virus-host interaction, demonstrating how HSV-1 modulates the cell response mediated by chemokines, such as CXCL10, CXCL11, CCL13, CCL2, and CCL4, and the receptor CMKLR1, to maintain a delicate balance with the host cell, thereby promoting viral persistence.

1. Introduction

Human Herpes Simplex viruses (HSVs) are among the oldest and best-adapted human pathogens [1]. They can escape the host's immune surveillance through a well-developed hide-and-seek mechanism as its evolutionary strategy. A non-specific defense initiates the host’s battle against the invading HSV-1 virion in primary infection. After the initial infection or relapse, virions are transported into the neuronal cell bodies in the trigeminal ganglia by retrograde axonal transport, resulting in a lifelong latent infection [2]. HSV-1 infection has minimal consequences for healthy adults. However, infection in infants or immuno-compromised individuals can develop fatal encephalitis, highlighting the importance of this phenomenon's corresponding immune response [3]. Indeed, the causes of such different outcomes following HSV-1 infection are unknown but involve the interplay between the virus and the immune response. Activated macrophages regulate the initial direct antiviral action of the host via the release of cytokines, tumor necrosis factor (TNF) and type I interferon (IFN-α) [4]. The host cytokines, TNF, and INF-1, in turn, induce natural-killer (NK) cells to release INF-γ. Their positive feedback with synergistic interactions collectively generates nitric oxide (NO) and reactive oxygen species (ROS) against the

invading virion [5]. Simultaneously, the combination of cytokines, macrophages, and other cells activates the immune cells to eliminate the pathogen. Chemotactic cytokines, as well as chemokines, play an important role in the development of immunological resistance to HSV-1 replication and act as a bridge between the innate and adaptive immune recognition of the pathogen and subsequent mobilization of leukocytes [6]. HSV-1 infection stimulates the production of various cytokines and chemokines, many of which act to suppress viral replication. In some instances, these products have contradictory outcomes based on the affected tissue site, while others require further study to determine their role. For instance, HSV-1 was shown to induce the secretion of CCL2, IL-8, IL-6, and TNF in primary genital endometrial epithelial cells [7]. In vivo, HSV promotes the expression of CXCL9 in the cervical mucus of HSV-positive women [8]. Importantly, CXCL9 and CXCL10 play a crucial role in preventing HSV-1 replication in central nervous system infections in a mouse model, likely through the recruitment of NK cells and cytotoxic T cells to infected tissues [9]. In addition, CXCL10 is considered a pivotal chemokine in orchestrating the recruitment of various leucocyte subsets such as CD4 and CD8 T cells, macrophages, dendritic cells, and NK cells to the CNS during HSV-1 infection [10]. Nevertheless, virus-mediated inhibition of other chemokines could favor the host. Indeed, CXCL2, which is secreted by monocytes in response to HSV, is known to recruit neutrophils that elicit damaging inflammatory immune responses to host cells and tissues, specifically neurons [11]. CXCL10 can also be induced by both IFN-γ and type I IFNs (IFN-α and IFN-β) [12]. However, the functional relevance of chemokine enhancement in the HSV life cycle and pathogenesis is still unknown. Data from our laboratory have demonstrated the effect of polyphenol-rich extracts from natural shelled (NPRE) pistachios kernels (Pistacia vera L.) on HSV-1 replication [13,14]. Besides, natural products and their derivatives, such as flavonoids and carotenoids, richly present in vegetables, fruits, cereals, nuts, herbs, seeds, stems, and flowers of numerous plants, possess numerous medicinal properties [15,16]. Particularly, flavonoids and carotenoids, which are abundant in plant-based foods, possess diverse biological activities, including anti-inflammatory properties [17,18]. These compounds can modulate inflammatory pathways by inhibiting the production of cytokines, chemokines and inflammatory enzymes [19,20]. At the same time, some studies have shown that carotenoids such as β-carotene, zeaxanthin and lycopene can regulate inflammatory pathways through MAPK and NF-kB, in endothelial cells [21–24]. Their antiviral effects and their influence on chemokine regulation in the context of HSV-1 replication remain largely unexplored. Monocytes play a central role in the host response contributing to antiviral immunity and inflammatory responses. These cells produce various pro-inflammatory cytokines and chemokines, including interleukin-1b, IL-1b; interleukin-6, TNF-a, and monocyte chemotactic protein-1, MCP-1 [25].While the antiviral property of carotenoids in this context, particularly through different inflammatory signal pathways, has not yet been proven, in our study, we will use a monocyte as an in *vitro* model for HSV-1 replication, and potentially an inducer of the cellular-mediated chemokine's response, to test the antiviral properties of natural extracts. Indeed, monocytes and macrophages play a crucial role in the immune response against HSV-1, contributing to a reduction in viral load in mouse model [6,26]. Understanding advances in the immunopathogenesis of HSV-1

infections is essential to these goals. In conclusion, these studies shed light on the idea that combination therapies for managing HSV-1 infections could be more effective than single therapies [27].

2. Results

2.1 Antiviral effects of NRRE and RURE on HSV-1 replication

To assess the direct impact of NRRE and RURE pistachio extracts (detailed in Materials and Methods section) on HSV-1 replication in monocytic THP-1 cells, a cytotoxicity assay was performed, as shown in Figure S1. The CC_{50} value is reported in Table S1, to determine the range within which the extracts can be used without causing harm or undesired effects. Based on the cytotoxicity results, THP-1 cells and the virus were pre-treated with concentrations of both NRRE and RURE extracts (0.4 and 0.6 mg/mL) below the toxic threshold (Fig. 1a). The effects of the extracts on different stages of the viral replication cycle were examined through multiple approaches, including viral titration, quantification of viral DNA, evaluation of representative viral transcripts by quantitative PCR analysis (qPCR), and detection of the viral protein ICP8 accumulation. The results indicated a dose-dependent reduction in viral plaques, suggesting a significant inhibitory effect of both NRRE and RURE extracts pretreatments (Fig. 1b). Furthermore, qPCR confirmed the decrease of HSV-1-DNA levels (Fig. 1c), reinforcing the antiviral activity of these extracts. The transcriptional analysis of key viral genes *ICP0* (alfa), *UL42* (beta), and *US11* (gamma) demonstrated marked downregulation following pretreatment with NRRE and RURE (Fig. 1d), indicating interference with the viral genetic cascade. Western blot analysis further revealed a significant reduction in ICP8 protein accumulation upon pretreatment with the extracts, as quantified through band intensity measurements normalized to GAPDH levels (Fig. 1e). Collectively, these findings demonstrate that NRRE and RURE effectively impair HSV-1 replication by targeting multiple stages of the viral replication program, highlighting their potential as novel antiviral agents.

2.2 Modulation of HSV-1-induced inflammatory chemokines by pistachio extracts in human monocytes.

Given monocytes' critical role in orchestrating immune responses, we first investigated whether HSV-1 replication actively induces chemokines and cytokines, in the presence or absence of NRRE and RURE extracts, in THP-1 cell lines. We analyzed cytokine and chemokine expression patterns in HSV-1-infected THP-1 cells, both untreated and treated with the extracts, using a Human Cytokines & Chemokines RT^2 Profiler PCR Array (Qiagen, Hilden, Germany). Expression profiles were compared (Fig. 2a). The array analysis revealed significant activation in immune-related gene expression following HSV-1 infection. The data were used to generate a heatmap, where red represents high expression and green indicates low expression in each sample. Out of the 84 human cytokines and chemokines analyzed (Table S3), 34 genes were upregulated, many of which are associated with immune cell recruitment and inflammation. Conversely, four genes were downregulated, including C5, a key component of the complement system, essential for innate immunity, ACKR2, an immune-regulatory chemokine receptor involved in chemokine

clearance and immune homeostasis and CCL23 and CCL28, chemokines involved in immune cell migration and mucosal immunity, respectively. These data suggest that HSV-1 not only triggers chemokines but may also actively suppress certain immune responses to establish the infection. Among the 34 genes upregulated by HSV-1 replication, 21 were significantly downregulated upon pretreatment with NRRE and RURE (Fig. 2b). These genes were categorized into three groups based on their chemokine motifs: -C-X-C motif chemokines: CXCL1, CXCL8, CXCL9, CXCL10, CXCL11, CXCL12, and CXCL13. -C-C motif chemokines: CCL2, CCL3, CCL4, CCL7, CCL8, CCL13, CCL24, and CCL26.-C-C motif chemokine receptors: CCR1, CCR4, CCR6, CCR7, CCRL1, and CMKLR1. Overall, our findings indicate that HSV-1 promotes a strong response by activating chemokines and cytokines during viral replication. At the same time, the pretreatment with NRRE and RURE extracts appears to downregulate key immune-regulatory genes associated with immune cell recruitment and inflammation (Fig. 2). To confirm these findings, the transcriptional levels of 6 the most representative chemokines (CCL2, CCL4, CCL13, CXCL10, CXCL11, CXCL13) and the receptor CMKLR1, were measured by qPCR (Fig. 3a). The findings agreed with the PCR array results (Fig. 2). Importantly, the results obtained by detecting the transcriptional levels of chemokines were confirmed by western blot analysis of some of them. In particular, the protein-accumulation of CXCL10 and CXCL13. The data demonstrated that the accumulation of CXCL10 and CXCL13 proteins, upon HSV-1 infection, was inhibited in treated THP-1-infected cells indicating that NRRE and RURE influence chemokine expression at both transcriptional (Fig. 3a) and translational levels (Fig. 3b lanes 5–6 *vs* lane 2).

2.3 HSV-1-mediated NF-κB activation is involved in regulating chemokines in THP-1-Infected cells.

One of the key regulators of pro-inflammatory genes, including those encoding chemokines and cytokines, is the NF-κB. It is well-established that HSV-1 recruits NF-κB during viral replication, most likely to ensure a favorable environment for viral survival [28,29]. Among the chemokines activated by HSV-1, CXCL10 possesses an upstream regulatory sequence that contains several critical regulatory elements for NF-κB and interferon-stimulated response element (ISRE), as well as sites for the binding of proteins such as heat shock (HS) factors [30]. Therefore, given that NRRE and RURE extracts reduce the expression of chemokines, such as CXCL10, CXCL11, CCL13, CCL2, CCL4, CCL13 and the receptor CMKLR1 activated by HSV-1, we hypothesized that these extracts exert their effects by targeting the HSV-1-mediated NF-κB activation. To test this, we measured NF-κB transcript levels in HSV-1-infected THP-1 cells in the presence or in the absence of NRRE and RURE (Fig. 4a). The results reported that HSV-1 infection caused a significant increase in NF-κB transcript levels (Fig. 4a), which correlates with the accumulation of the phosphorylated form of p65, as shown in Fig. 4b lane 2. In contrast, the pretreatment of HSV-1-infected THP-1 cells with NRRE and RURE significantly reduces the NF-κB transcript levels (Fig. 4a) and the phosphorylation of p65 protein (Fig. 4b lane 2 *vs* lanes 5 and 7). These data suggest that these natural compounds effectively inhibit NF-κB activation induced by HSV-1 infection.

2.3 Zeaxanthin inhibits chemokine expression in HSV-1-infected THP-1 cells.

Previous studies have reported that the pure compound zeaxanthin, a carotenoid present in pistachio extracts, exhibits antiviral activity against HSV-1 in infected cells [14]. Therefore, we have investigated the specific effects of zeaxanthin on chemokine expression during HSV-1 replication. To this purpose, THP-1 cells and HSV-1 were pretreated with zeaxanthin (10 µM) for 1 hour at 37°C. Following pretreatment, the virus was used to infect THP-1 cells at a multiplicity of infection (MOI) of 50. One-hour post-infection, the viral inoculum was removed and replaced with a growth medium containing zeaxanthin (10 µM). At 24 hours post-infection, total RNA was extracted and analyzed using quantitative real-time PCR to measure the transcript levels of chemokines CCL2, CCL4, CC13, CXCL10, CXCL11, CXCL13 and CMKRL1. The results showed that zeaxanthin significantly reduces the levels of chemokine upregulated by HSV-1, as evidenced by the decreased transcriptional levels of CCL2, CCL4, CC13, CXCL10, CXCL11, CXCL13 and CMKRL1 (Fig. 5a). To note, CXCL10 protein levels were reduced following HSV-1 zeaxanthin treatment (Fig. 5b, lane 2 *vs.* 4), as a consequence a significant reduction of US11 viral protein accumulation (Fig. 5b, lane 2 *vs.* 4) and the representative viral transcripts of the HSV-1 gene cascade *ICP0 (α gene), UL42 (β gene), US11 (γ gene*) were observed (Fig. 5c). To confirm the results obtained with NRRE and RURE, we also tested the ability of zeaxanthin to inhibit the accumulation of NF-κB transcript levels. Figure 5d shows that zeaxanthin effectively inhibits the HSV-1-mediated transcriptional activation of NF-kB, which correlates with a decrease in the transcriptional levels of chemokines.

2.4 Chemokine accumulation is strictly dependent on HSV-1 replication and virus-induced NF-κB activation.

The data reported up to this point demonstrate that HSV-1 induces a strong activation of chemokine response in host immune cells, by recruiting the NF-κB. However, it remains unclear whether the expression of these chemokines depends solely on viral entry or also requires active viral replication. Additionally, it remains unclear whether HSV-1-induced chemokine expression is a direct consequence of NF-κB activation or if it occurs independently.

Therefore, to determine whether chemokine induction depends on viral replication, THP-1 cells were infected in the presence of phosphonoacetic acid (PAA, 300 µg/mL), an inhibitor of HSV-1 DNA polymerase. PAA treatment significantly reduced the accumulation of all measured chemokine transcripts (CXCL10, CXCL11, CCL13, CCL2, CCL4, CCL13 and CMKLR1) compared to untreated infected controls (Fig. 6a), indicating that active viral replication is required for the full induction of chemokines. To confirm the inhibitory effect of PAA on viral replication, we assessed the mRNA levels of Us11, a late viral gene whose expression depends on newly synthesized viral DNA and is therefore blocked when DNA replication is inhibited [31]. PAA treatment resulted in a substantial decrease in Us11 transcripts (Fig. 6b), validating that the observed reduction in chemokine expression was associated with impaired HSV-1 replication. In addition, the protein levels of CXCL10 and the activation of NF-κB were also

monitored by Western blot analysis (Fig. 6c). Consistent with the transcriptional data, protein levels of CXCL10 were markedly reduced upon PAA treatment, indicating that their induction is dependent on HSV-1 replication (Fig. 6c lane 2 *vs* lane 4). Moreover, the expression of phosphorylated NF-κB p65, which was strongly increased in infected THP-1 cells, as also shown in Fig. 4b lane 2, was drastically reduced upon PAA treatment (Fig. 6c, lane 2 *vs* 4). These findings further support the conclusion that NF-κB activation is closely linked to viral replication and is significantly impaired when HSV-1 DNA synthesis is inhibited.

To investigate the role of NF-κB, we compared chemokine expression in parental THP-1 cells with chemokine expression in THP-dnIKBa cells, which are engineered to inhibit NF-κB activation [29].

HSV-1 infection in THP-dnIκBα cells resulted in a significant reduction in chemokine mRNA levels compared to wild-type THP-1 cells (Fig. 6d), indicating that NF-κB is a critical driver of HSV-1-induced chemokine transcription. Notably, the chemokine suppression mediated by NF-κB inhibition rescued HSV-1 replication. Indeed, in THP-dnIκBα cells, a significant increase in mRNA levels of key viral genes, including ICP0, UL42, and Us11, was observed compared to infected wild-type THP-1 cells (Fig. 6e), suggesting that the inhibition of NF-κB recruitment supports HSV-1 replication, presumably by promoting a proviral cellular environment.

3. Conclusion

This study demonstrates that *Pistacia vera* L. extracts, specifically NRRE and RURE, exert potent antiviral effects against HSV-1 infection in monocytic THP-1 cells. Treatment with non-cytotoxic concentrations of the extracts significantly reduced HSV-1 replication, as evidenced by decreased viral titers, reduced levels of viral DNA, massive reduction in the accumulation of key viral gene transcripts (ICP0, UL42, US11), and diminished accumulation of the viral protein ICP8. These data support the conclusion that NRRE and RURE interfere with multiple stages of the HSV-1 replication cycle as demonstrated in a previous study using the Vero cellular model [14]. We further show that HSV-1 infection elicits a robust cellular response, characterized by the upregulation of a wide array of chemokines and cytokines, including CCL2, CCL4, CCL13, CXCL10, CXCL11, CXCL13, and the receptor CMKLR1. Notably, many of these genes were significantly downregulated upon pretreatment with NRRE and RURE, suggesting that the influence of these extracts may contribute to their antiviral activity. Zeaxanthin, a bioactive compound present in pistachios [14], also downregulates the expression of CCL2, CCL4, CCL13, CXCL10, CXCL11, CXCL13, and the receptor CMKLR1, resulting in reduced viral genes expression and proteins production, further supporting this mechanism. Moreover, our findings indicate that chemokine induction by HSV-1 is strictly dependent on both active viral replication and NF-κB. Indeed, inhibition of HSV-1 replication by PAA, or blocking NF-κB activation using THP-1-dnIκBα, reduces the accumulation of chemokine transcripts (Fig. 6). In line with our observations, a similar response regarding CCL4 expression has been documented in U937-dnIκBα cells 24 hours post-infection, further supporting the critical role of NF-κB in regulating this chemokine during HSV-1 replication [32]. Thus, while NF-κB activation leads to a robust induction of multiple chemokines, suppressing NF-κB, results in decreased

levels of chemokines. However, this event does not suppress viral replication and may even enhance it. On the other hand, elevated NF-κB and chemokine levels coexist with active viral replication. This paradox suggests that the activation of chemokines during HSV-1 infection may serve dual and context-dependent roles, both antiviral and proviral, and that the virus may exploit the host's response to its advantage [6]. Indeed, while chemokine upregulation is typically associated with antiviral immune responses, our findings, along with those of others, suggest that specific chemokines may play a proviral role. For example, CXCL10 and CCL2, though known for recruiting immune effector cells, can paradoxically promote viral spread by attracting permissive or inflammatory cells to the site of infection [33]. CXCL10 is upregulated in infected corneal and neuronal tissues. It supports immune cell recruitment, but excessive or dysregulated chemokine production may exacerbate tissue damage and facilitate viral dissemination through a mechanism dependent on cellular PKR and viral ICP0 [34]. These findings reinforce the idea that the virus may tolerate or even benefit from a certain level of chemokines or access immune cells to facilitate spread or modulate the immune environment. During HSV-1 infection, the engagement of TLR2 mediates the production of CCL2 in infected neurons, thereby coordinating the recruitment of macrophages [26]. HSV-1 and HSV-2 induced expression of the CC chemokine RANTES/CCL5 in murine macrophage cell lines and peritoneal cells [35]. A non-directed link between HSV-1 and CMKLR1 has been identified so far. However, its expression and activity are modulated in HIV, where CMKLR1 signaling is involved in viral control through the recruitment of plasmacytoid dendritic cells [36]. It has been proposed to function as a minor co-receptor, promoting infection by selecting HIV and SIV isolates [37]. In other viral models, chemokine-mediated proviral effects have also been described. For instance, HIV-1 uses CCR5 and CXCR4 as coreceptor, and chemokines that bind these receptors can paradoxically enhance infection under certain conditions [38]. In influenza A virus infection, CCL2 has been shown to exacerbate lung pathology and enhance viral spread by recruiting inflammatory monocytes [39]. These findings emphasize that chemokine production, although part of the host defense, can be subverted by viruses to support their own replication and persistence. In the case of HSV-1, the potential benefit of chemokine potentiation is currently unknown. Existing hypotheses include the recruitment of more cells susceptible to infection to the site of infection and the induction of an activated proviral state in neighboring cells [40]. Our data show that the chemokine storm is not only a consequence of infection but an NF-κB-dependent, virus-facilitated process that may be proviral. In summary, the induction of chemokines and the recruitment of NF-κB during HSV-1 replication reflect a complex interplay between these factors. However, they may also be co-opted by HSV-1 to facilitate replication and spread. The paradoxical effect in the cellular model in which NF-κB is blocked (THP-1-dnIκBα), resulting in a reduction of chemokines with subsequent increase in viral replication, may reveal that the chemokine-induced immune response imposes partial control on the virus and that HSV-1 has developed mechanisms to balance. Further studies are necessary to elucidate the specific role of individual chemokines in HSV-1 infection, as their diverse functions may differentially influence viral replication, immune cell recruitment, and tissue inflammation. In conclusion, our study highlights the potential of *Pistacia vera* L. -derived compounds as promising dual-action agents that target both HSV-1 replication and the associated cellular response. Therefore, based on our findings and literature data, we propose a

mechanism to describe the impact of viral replication on monocytes characterized by upregulation of several chemokines involved in viral pathogenesis and immune activation (Fig. 7a). Natural compounds, such as *Pistacia vera* L. extracts (NRRE and RURE) and zeaxanthin, which interfere with viral replication, have, as a consequence, the attenuation of chemokine-mediated immune activation (Fig. 7b). These dual effects may have therapeutic relevance in managing herpetic-related complications, especially in immune-privileged or highly sensitive tissues, such as the brain, eyes, and genital tract, where inflammation significantly contributes to pathology.

4. Materials and Methods

4.1 Cells and virus

THP-1 (human acute monocytic leukemia) and VERO (African green monkey kidney), were all originally obtained from ATCC (https://www.atcc.org/). THP-1 were cultured in RPMI-1640 medium supplemented with 10% FBS (Euroclone), 1mM Sodium Pyruvate (Sigma-Aldrich), 10 mM Hepes buffer (Sigma-Aldrich). DN IκBα THP-1 cells, stably transfected with a dominant negative mutant IκBα[29] were cultured in RPMI-1640 medium and maintained under selection with 400 µg/ml of Geneticin (Gibco).

VERO cells were cultured in Dulbecco's Modified Eagle's High Glucose Medium (DMEM, Euroclone, Pero, MI, Italy) supplemented with 6% fetal bovine serum (FBS).

All mediums are supplemented with 100 U/mL penicillin, and 100 mg/mL streptomycin (Lonza, Belgium). All cell lines were grown at 37°C in a 5% CO2 incubator.

The prototype HSV-1 (F) strain, used for the in vitro experiments, was kindly provided by Dr. Bernard Roizman (University of Chicago, Chicago, IL, USA), and the virus stock was produced and titered in Vero cells.

4.2 Materials

Californian natural raw polyphenols-rich extract (NRRE, Pistacchi Sgusciati California Pissgsu01/BSV1, L67316221262) and roasted unsalted polyphenols-rich extract (RURE, Pistacchi Sgusciati Tostati California Pissgstu01/BSV1) pistachio polyphenols-rich extracts were kindly supplied by the American Pistachio Growers (Fresno, CA, USA). NRRE or RURE (10 g) were extracted with n-hexane as previously described [14]and the quantification of phenolic compounds was performed by RP-HPLC-DAD.

4.3 Antibodies and reagents

Primary antibodies used included GAPDH (sc-32233), α Tubulin (DM1A) (sc-32293), CXCL10 (sc-101500), and CXCL13 (sc-73740) from Santa Cruz Biotechnology; ICP8 and US11, kindly provided by Professor Bernard Roizman; β-actin (ab8226) from Abcam; and phospho-NF-κB p65 (Ser536) (#3033) from Cell Signaling Technology. HRP-conjugated goat anti-mouse and anti-rabbit IgG secondary antibodies were obtained from Merck Millipore.

Phosphonoacetic acid (PAA) from Sigma-Aldrich, was used as an inhibitor of DNA synthesis in HSV-infected cells and was dissolved in the medium and used at 300 µg/mL during and after HSV-1 adsorption [41].

4.4 Viability Assay

To evaluate cell viability after exposure to pistachio extracts, the ViaLight™ Plus Cell Proliferation and Cytotoxicity Bioassay (Lonza Group Ltd., Basel, Switzerland) was utilized. THP-1 cells were plated in 96-well microplates and treated with different concentrations of NRRE and RURE (0.8, 0,6, 0.4, 0,3 and 0.2 mg/mL) for a duration of 72 hours. Following the incubation period, cell viability was determined using the GloMax® Multi Microplate Luminometer (Promega Corporation, Madison, WI, USA) in conjunction with the ViaLight™ Plus assay, which detects luminescence generated from ATP breakdown.

The luminescent signals were subsequently translated into a cell viability percentage using the following formula:

Cell viability (%) = (A - B) / (C - B)

where:

A represents the mean luminescence of treated samples,

B denotes the background luminescence, and

C is the mean luminescence of untreated control samples.

4.5 Pre-treatment and infection protocol in THP-1 cells

THP-1 cells were seeded in appropriate culture flasks and maintained under standard conditions. Prior to infection, both the THP-1 cells and the HSV-1 viral suspension were separately pre-treated with NRRE, RURE, and zeaxanthin at various concentrations, depending on the specific experimental setup. The pre-treatment was carried out for 1 hour at 37°C. Following this step, THP-1 cells were infected with the HSV-1 virus at a multiplicity of infection (MOI) of 50, using the virus that had been previously exposed to NRRE, RURE, and zeaxanthin. Infection was allowed to proceed for 1 hour at 37°C. After the infection period, the viral inoculum was carefully removed, and the cells were washed with growth medium to eliminate residual unbound virus. Fresh growth medium containing NRRE, RURE, and zeaxanthin at the same concentrations used during the pre-treatment phase was then added to the cells. The samples were incubated for an additional 24 hour post-infection (p.i.) and were then collected and processed for subsequent analyses, depending on the objectives of each experimental condition (e.g., reduction plaque assay, gene expression analysis, or protein quantification).

4.6 Standard Plaque Assay on VERO cells.

The plaque assay was carried out using VERO cells. Infected, treated, and untreated THP-1 cells, along with their supernatants, were subjected to three freeze-thaw cycles. Subsequently, 100 µL of each viral

suspension dilution was used to infect VERO cell monolayers. The infection was conducted under gentle agitation for 1 hour at 37°C. After incubation, the viral inoculum was removed and replaced with culture medium containing 0.8% methylcellulose. After 72 hours, viral plaques were visualized and counted under a microscope following staining with a crystal violet solution.

4.7 Western Blot Analysis

An Immunoblot analysis was performed to assess the accumulation of viral proteins, as previously described [41]. Briefly, total cell lysates were prepared by resuspending cells in 1X SDS sample buffer (62.5 mM Tris-HCl, pH 6.8; 50 mM dithiothreitol (DTT); 10% glycerol; 2% sodium dodecyl sulfate (SDS); 0.01% Bromophenol Blue; 1X EDTA-free Protease Inhibitor Cocktail (Roche). The samples were then boiled for 5 minutes. Equal amounts of protein were separated on gels containing different percentages of SDS-polyacrylamide, 15% to resolve CXCL10 and CXCL13, and 10% to resolve phospho-NF-κB p65 and transferred to nitrocellulose membrane. After incubation in blocking buffer (5% non-fat dry milk in TBS) at 37°C, membranes were probed overnight with specific primary antibodies and then incubated with secondary antibodies. Immunoreactive bands were visualized using the LiteUP WB Chemiluminescent Substrate (Euroclone) and captured using a ChemiDoc Touch Imaging System (Bio-Rad) where indicated. Quantification of band intensities was conducted using ImageJ software and Bio-Rad Image Lab 6 software. Target protein levels were normalized to housekeeping, and results were graphically represented using GraphPad Prism 8 (GraphPad Software, San Diego, CA, USA).

4.8 Viral DNA Extraction and Real-Time PCR

Viral DNA was extracted using TRIzol® (Thermo Fisher Scientific, Waltham, MA, USA) according to the manufacturer's instructions.

The procedure, based on the phenol/chloroform extraction method, allows for the precipitation of viral DNA from the organic phase [42]. The DNA pellet was washed twice in a solution containing 0.1 M trisodium citrate in 10% ethanol and then dissolved in 8 mM NaOH. The concentration of DNA was determined by fluorometer analysis with the Qubit double-stranded DNA (dsDNA) HS (High Sensitivity) Assay Kit according to the manufacturer's instructions. The amplification of viral DNA was carried out by TaqMan™Universal Master Mix II (Applied Biosystems™, Foster City, CA, USA) in a 50 µL reaction mixture containing the following: TaqMan Universal Master Mix II, DNA (100 ng); HSV-1 forward (10 µM) and HSV-1 reverse (10 µM) primers (Table S2); and the TaqMan probe (5 µM) (Table S2). The amplification was carried out on Applied Biosystems 7300 Real-Time PCR System under the following conditions: 10 min at 95°C, 60 s at 95°C for 40 cycles, 30 s at 60°C, and 30 s at 72°C. Each amplification run contained one negative control. The primers were designed on a large catalytic subunit of HSV-1 DNA polymerase holoenzyme (UL30 gene). The relative quantitation of HSV-1 DNA was generated by the comparative Ct method using GAPDH as a housekeeping gene (Table S2). One-way analysis of variance (ANOVA) and the GraphPad Prism 6 software (GraphPad Software, San Diego, CA, USA) was used to perform statistical analysis and graphical representations, respectively.

4.9 RNA Extraction, Reverse Transcription, and Real-Time PCR

Total RNA was extracted using TRIzol® (Life Technologies, Carlsbad, USA), according to the manufacturer's instructions, and DNase-treated before cDNA transcription as follows: 1 µg of RNA was incubated at 37°C for 2 h with 5 µL 10X DNase I Buffer, 2 µL Recombinant RNase-free DNase I (10U) (2270A TaKaRa, Dalian, China) and RNase inhibitor (20U) (N251A Promega). The procedures were published previously [43]. The concentration of extracted RNA was determined using Qubit™ RNA HS Assay (Invitrogen). Total RNA (0.5µg) was reverse transcribed using avian myeloblastosis virus reverse transcriptase (Promega, Madison, WI) under the following conditions: denaturation at 70°C for 10 min, followed by 42°C for 45 min, 52°C for 45 min and 95°C for 5 min. The cDNAs were used for quantitative Real-Time PCR by using QuantiNova SYBR Green PCR Kit (Qiagen) carried out on Qiagen QIAquant 96 2plex PCR Thermal Cycler. The thermal profile consists of a 2 min incubation at 95°C followed by 40 cycles of 5 sec denaturation at 95°C, 10 s annealing/extension at 60°C. The cDNA copy numbers were normalized to GAPDH. The analytic primers for RT-PCR are reported in Table S2. Each quantitative Real-time PCR experiment includes a minus-reverse transcriptase control.

4.10 RT2 Profiler PCR Arrays

A total of 750 ng of cDNA was used for the RT² Profiler PCR Array (QIAGEN, Cat. no. PAHS-033Z), in combination with the RT² SYBR® Green qPCR Mastermix (Cat. no. 330502) in RNase/DNase-free water. Equal volumes (25 µL) of the reaction mixture were dispensed into each well of the array plate, which contained pre-aliquoted, gene-specific primer sets. PCR amplification and detection were carried out using the Applied Biosystems 7300 Real-Time PCR System (Applied Biosystems, Carlsbad, CA, USA) with the following thermal cycling conditions: initial denaturation at 95°C for 10 minutes, followed by 40 cycles of 15 seconds at 95°C (denaturation) and 60 seconds at 60°C (annealing/extension).

Each 96-well plate included controls for genomic DNA contamination, reverse transcription efficiency, and PCR performance. Glyceraldehyde-3-phosphate dehydrogenase (GAPDH) served as the reference (housekeeping) gene. Data analysis was performed using the Qiagen GeneGlobe online platform, comparing all experimental conditions: infected vs. uninfected and treated vs. untreated samples. A cycle threshold (Ct) value of 35 was used as the cut-off for detectable gene expression. Supplementary Table S3 presents the gene expression profiles of HSV-1-infected THP-1 cells, either untreated or treated with NRRE and RURE, in comparison to uninfected, untreated controls.

4.11 Statistical Analysis

Data are presented as mean ± standard deviation (SD) from at least three independent experiments. Statistical analysis was performed using GraphPad Prism version 8.0.1 (GraphPad Software Inc., San Diego, CA, USA) through one-way analysis of variance (ANOVA). Array data were calculated using values for three technical and one biological replicates. For qPCR analysis, means ± standard deviations were calculated from two biological replicates and three technical replicates. The EC50 values were

calculated from dose inhibition curves using nonlinear regression analysis by GraphPad Prism and are reported in Table S1.

Declarations

Acknowledgements

We are deeply grateful to Professor Bernard Roizman for his invaluable scientific support and for inspiring us to explore the hidden world behind HSV infection, shaping our research with his insight and passion.

Author contributions

Conceptualization: M.T.S., G.M. and R.P.; software: R.P.; investigation: R.P., P.T., M.P.T and M.C; data curation: R.P.; and M.T.S., supervision: M.T.S., G.M. and R.P.; project administration: M.T.S. and G.M.; funding acquisition: M.T.S. and G.M. All authors have read and agreed to the published version of the manuscript.

Data availability statement (mandatory)

All data supporting the findings of this study are included in the article and its supplementary materials

Competing interests

The authors declare no competing interests.

Funding

This work was funded by American Pistachio Growers (APG), Fresno, CA (USA).

References

1. Arvin A, C.-F. G. M. E. M. P. R. B. W. R. Y. K. editors. *Human Herpesviruses: Biology, Therapy, and Immunoprophylaxis.* (2007).
2. Whitley, R. J. & Roizman, B. Herpes simplex virus infections. *The Lancet* **357**, 1513–1518 (2001).
3. Saleh D, Y. S. S. S. Herpes Simplex Type 1. *https://www.ncbi.nlm.nih.gov/books/NBK482197/* (2025).
4. Toews, G. B. Macrophages. in *Asthma and COPD* 133–143 (Elsevier, 2009). doi:10.1016/B978-0-12-374001-4.00011-0.
5. Ellermann-Eriksen, S. Macrophages and cytokines in the early defence against herpes simplex virus. *Virol J* **2**, 59 (2005).
6. Smith, J. B., Herbert, J. J., Truong, N. R. & Cunningham, A. L. Cytokines and chemokines: The vital role they play in herpes simplex virus mucosal immunology. *Front Immunol* **13**, (2022).

7. Wang, L., Wang, R., Xu, C. & Zhou, H. Pathogenesis of Herpes Stromal Keratitis: Immune Inflammatory Response Mediated by Inflammatory Regulators. *Front Immunol* **11**, (2020).
8. Thapa, M., Welner, R. S., Pelayo, R. & Carr, D. J. J. CXCL9 and CXCL10 Expression Are Critical for Control of Genital Herpes Simplex Virus Type 2 Infection through Mobilization of HSV-Specific CTL and NK Cells to the Nervous System. *The Journal of Immunology* **180**, 1098–1106 (2008).
9. Shin, H. & Iwasaki, A. A vaccine strategy that protects against genital herpes by establishing local memory T cells. *Nature* **491**, 463–467 (2012).
10. Hussain, M. S. *et al.* Immunopathology of herpes simplex virus-associated neuroinflammation: Unveiling the mysteries. *Rev Med Virol* **34**, (2024).
11. Suazo, P. A. *et al.* Evasion of Early Antiviral Responses by Herpes Simplex Viruses. *Mediators Inflamm* **2015**, (2015).
12. McKimmie, C. & Michlmayr, D. Role of CXCL10 in central nervous system inflammation. *Int J Interferon Cytokine Mediat Res* 1 (2014) doi:10.2147/IJICMR.S35953.
13. Musarra-pizzo, M. *et al.* In vitro anti-HSV-1 activity of polyphenol-rich extracts and pure polyphenol compounds derived from pistachios kernels (Pistacia vera l.). *Plants* **9**, (2020).
14. Pennisi, R. *et al.* Mechanistic Understanding of the Antiviral Properties of Pistachios and Zeaxanthin against HSV-1. *Viruses* **15**, 1651 (2023).
15. Zheng, X., Zhang, X. & Zeng, F. Biological Functions and Health Benefits of Flavonoids in Fruits and Vegetables: A Contemporary Review. *Foods* **14**, 155 (2025).
16. Yi, Y.-S. Regulatory Roles of Flavonoids in Caspase-11 Non-Canonical Inflammasome-Mediated Inflammatory Responses and Diseases. *Int J Mol Sci* **24**, 10402 (2023).
17. Al-Khayri, J. M. *et al.* Flavonoids as Potential Anti-Inflammatory Molecules: A Review. *Molecules* **27**, 2901 (2022).
18. Saini, R. K., Nile, S. H. & Park, S. W. Carotenoids from fruits and vegetables: Chemistry, analysis, occurrence, bioavailability and biological activities. *Food Research International* **76**, 735–750 (2015).
19. Leyva-López, N., Gutierrez-Grijalva, E., Ambriz-Perez, D. & Heredia, J. Flavonoids as Cytokine Modulators: A Possible Therapy for Inflammation-Related Diseases. *Int J Mol Sci* **17**, 921 (2016).
20. Ribeiro, D., Freitas, M., Lima, J. L. C. & Fernandes, E. Flavonoids inhibit the production of cytokines/chemokines and induce apoptosis in human neutrophils. *Free Radic Biol Med* **75**, S46 (2014).
21. Bai, S.-K. *et al.* β-Carotene inhibits inflammatory gene expression in lipopolysaccharide-stimulated macrophages by suppressing redox-based NF-κB activation. *Exp Mol Med* **37**, 323–334 (2005).
22. Di Tomo, P. *et al.* β-Carotene and lycopene affect endothelial response to TNF-α reducing nitro-oxidative stress and interaction with monocytes. *Mol Nutr Food Res* **56**, 217–227 (2012).
23. Li, R., Hong, P. & Zheng, X. β-carotene attenuates lipopolysaccharide-induced inflammation via inhibition of the NF-κB, JAK2/STAT3 and JNK/p38 MAPK signaling pathways in macrophages.

Animal Science Journal **90**, 140–148 (2019).

24. Lin, H.-W. *et al.* Regulation of virus-induced inflammatory response by β-carotene in RAW264.7 cells. *Food Chem* **134**, 2169–2175 (2012).
25. Dash, S. P., Gupta, S. & Sarangi, P. P. Monocytes and macrophages: Origin, homing, differentiation, and functionality during inflammation. *Heliyon* **10**, e29686 (2024).
26. Brun, P. *et al.* Herpes Simplex Virus Type 1 Engages Toll Like Receptor 2 to Recruit Macrophages During Infection of Enteric Neurons. *Front Microbiol* **9**, (2018).
27. Garber, A., Barnard, L. & Pickrell, C. Review of Whole Plant Extracts With Activity Against Herpes Simplex Viruses In Vitro and In Vivo. *J Evid Based Integr Med* **26**, (2021).
28. TERESA SCIORTINO, M. *et al.* Signaling Pathway Used by HSV-1 to Induce NF-κB Activation. *Ann N Y Acad Sci* **1096**, 89–96 (2007).
29. Venuti, A. *et al.* HSV-1\EGFP stimulates miR-146a expression in a NF-κB-dependent manner in monocytic THP-1 cells. *Sci Rep* **9**, (2019).
30. Elemam, N., Talaat, I. & Maghazachi, A. CXCL10 Chemokine: A Critical Player in RNA and DNA Viral Infections. *Viruses* **14**, 2445 (2022).
31. Honess, R. W. & Watson, D. H. Herpes simplex virus resistance and sensitivity to phosphonoacetic acid. *J Virol* **21**, 584–600 (1977).
32. Marino-Merlo, F. *et al.* HSV-1-induced activation of NF-κB protects U937 monocytic cells against both virus replication and apoptosis. *Cell Death Dis* **7**, e2354–e2354 (2016).
33. Carr, D. J. J., Chodosh, J., Ash, J. & Lane, T. E. Effect of Anti-CXCL10 Monoclonal Antibody on Herpes Simplex Virus Type 1 Keratitis and Retinal Infection. *J Virol* **77**, 10037–10046 (2003).
34. Carr, D. J. J. & Tomanek, L. Herpes Simplex Virus and the Chemokines That Mediate the Inflammation. in *Chemokines and Viral Infection* 47–65 (Springer Berlin Heidelberg, Berlin, Heidelberg). doi:10.1007/978-3-540-33397-5_3.
35. Melchjorsen, J., Pedersen, F. S., Mogensen, S. C. & Paludan, S. R. Herpes Simplex Virus Selectively Induces Expression of the CC Chemokine RANTES/CCL5 in Macrophages through a Mechanism Dependent on PKR and ICP0. *J Virol* **76**, 2780–2788 (2002).
36. Yoshimura, T. & Oppenheim, J. J. Chemokine-like receptor 1 (CMKLR1) and chemokine (C–C motif) receptor-like 2 (CCRL2); Two multifunctional receptors with unusual properties. *Exp Cell Res* **317**, 674–684 (2011).
37. Samson, M. *et al.* ChemR23, a putative chemoattractant receptor, is expressed in monocyte-derived dendritic cells and macrophages and is a coreceptor for SIV and some primary HIV-1 strains. *Eur J Immunol* **28**, 1689–1700 (1998).
38. Faivre, N., Verollet, C. & Dumas, F. The chemokine receptor CCR5: multi-faceted hook for HIV-1. *Retrovirology* **21**, 2 (2024).
39. Lai, C. *et al.* C-C Motif Chemokine Ligand 2 (CCL2) Mediates Acute Lung Injury Induced by Lethal Influenza H7N9 Virus. *Front Microbiol* **8**, (2017).

40. Pontejo, S. M., Murphy, P. M. & Pease, J. E. Chemokine Subversion by Human Herpesviruses. *J Innate Immun* **10**, 465–478 (2018).
41. Colao, I. *et al.* The ERK-1 function is required for HSV-1-mediated G1/S progression in HEP-2 cells and contributes to virus growth. *Sci Rep* **7**, (2017).
42. Pennisi, R. *et al.* Analysis of Antioxidant and Antiviral Effects of Olive (Olea europaea L.) Leaf Extracts and Pure Compound Using Cancer Cell Model. *Biomolecules* **13**, 238 (2023).
43. Pennisi, R. & Sciortino, M. HSV-1 Triggers an Antiviral Transcriptional Response during Viral Replication That Is Completely Abrogated in PKR−/− Cells. *Pathogens* **12**, 1126 (2023).

Figures

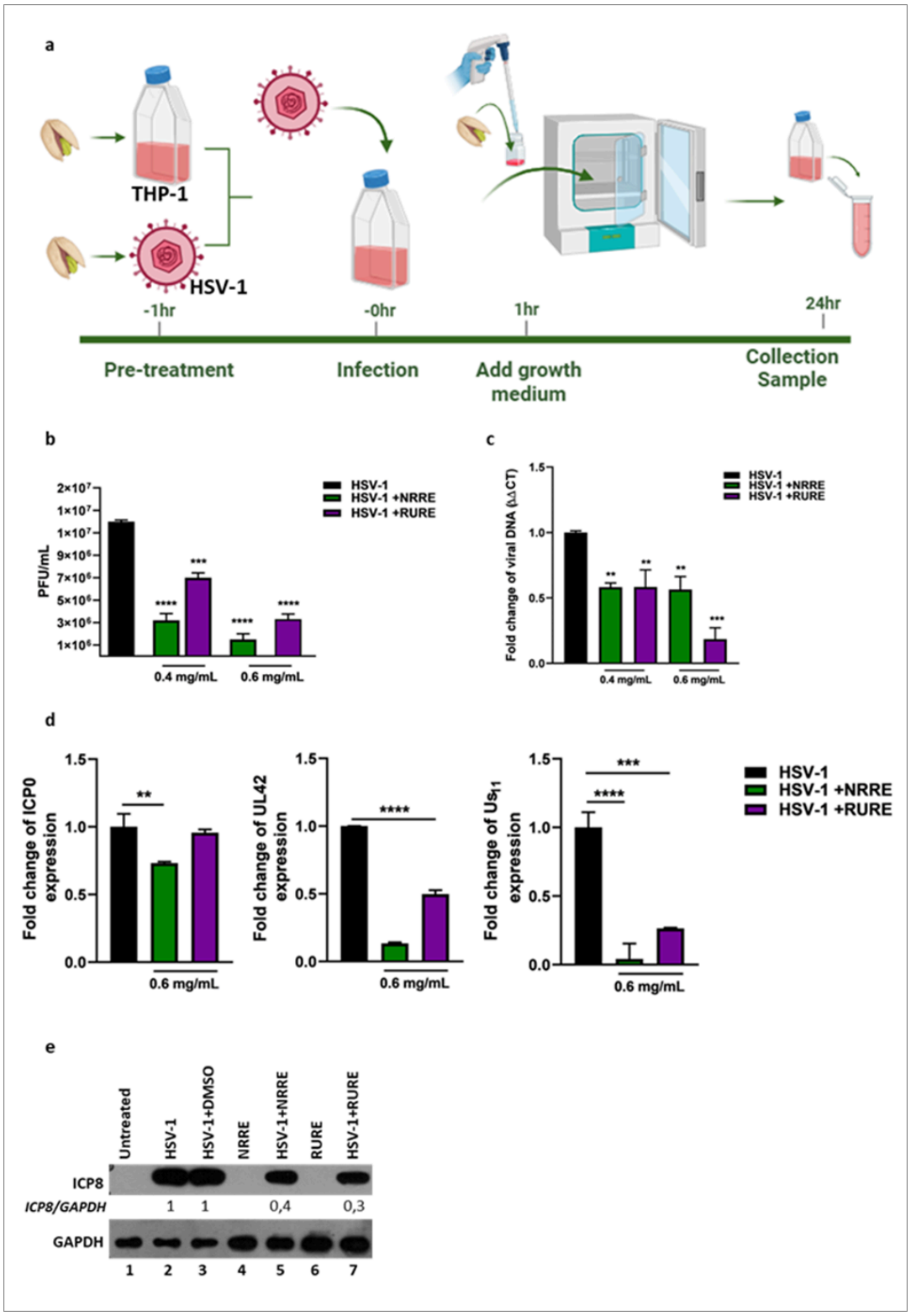

Figure 1

Antiviral effect of NRRE and RURE pretreatment on HSV-1 replication. a) Graphical representation of the experimental workflow: THP-1 cells and virus were pre-treated with NRRE and RURE at 0.4 and 0.6 mg/mL for 1h at 37 °C and then infected at 50 MOI with pretreated HSV-1 at 37°C. Thus, 1h later the viral inoculum was removed and replaced with a growth medium containing NRRE and RURE at 0.4 and 0.6 mg/mL. Samples were collected at 24h p.i and processed for further analysis. b) Evaluation of viral title

in THP-1 cells following NRRE and RURE pretreatment. Infected and uninfected, treated, and untreated THP-1 cells were frozen and thawed three times and 100 µl of each dilution of the viral suspension was used to infect the VERO monolayers. The multiwell plates were incubated for 1h at 37°C. Then, the viral inoculum was removed and replaced with a culture medium containing 0.8% methylcellulose. After 72h the plaques were visualized and counted at the microscope after staining with a crystal violet solution. c-d) Infected and uninfected, treated, and untreated THP-1 cells were collected 24h p.i and processed for viral DNA detection (panel c) and mRNA extraction and quantitative Real-time PCR to analyse ICP0, UL42, and Us11 viral transcripts as representative genes of the sequential genetic cascade of HSV-1 (panel d). Relative quantization of viral DNA and genes was performed using real-time quantitative PCR and analysed by the comparative Ct method (ΔΔCt). Data are expressed as a mean (± SD) of at least three experiments and asterisks (*, **, ***) indicate the significance of p-values less than 0.05, 0.01, and 0.001, respectively. e) Western blot analysis was performed to detect the levels of ICP8, as a representative viral protein.

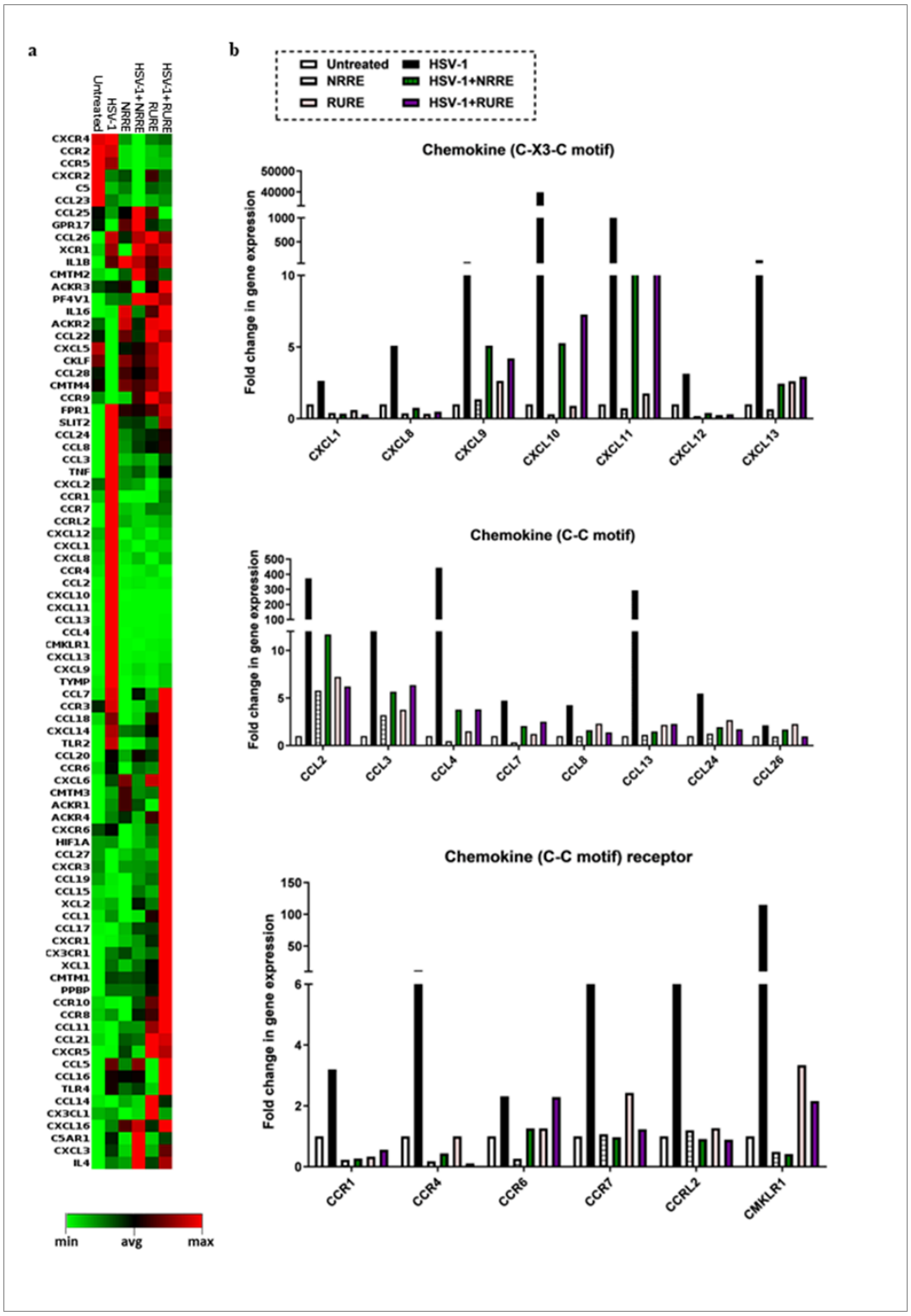

Figure 2

Expression profile of cytokines and chemokines in THP-1 cells infected with HSV-1 and treated with NRRE and RURE. THP-1 cells and virus were pre-treated with NRRE and RURE at 0.6 mg/mL for 1h at 37 °C and then infected at 50 MOI with pre-treated HSV-1 at 37°C. 1h later the viral inoculum was removed and replaced with a growth medium in the presence of NRRE and RURE at 0.6 mg/mL. The total RNA was extracted 24h p.i. and reverse transcribed to obtain cDNA. a-b) Expression data of cytokines and

chemokines in the THP-1 cells were measured performing a DNA array (Human Cytokines & Chemokines RT2 Profiler PCR Array; Qiagen) and expressed as relative mRNA normalized to untreated and uninfected THP-1. The chemokines were classified into 3 groups as reported in panel b.

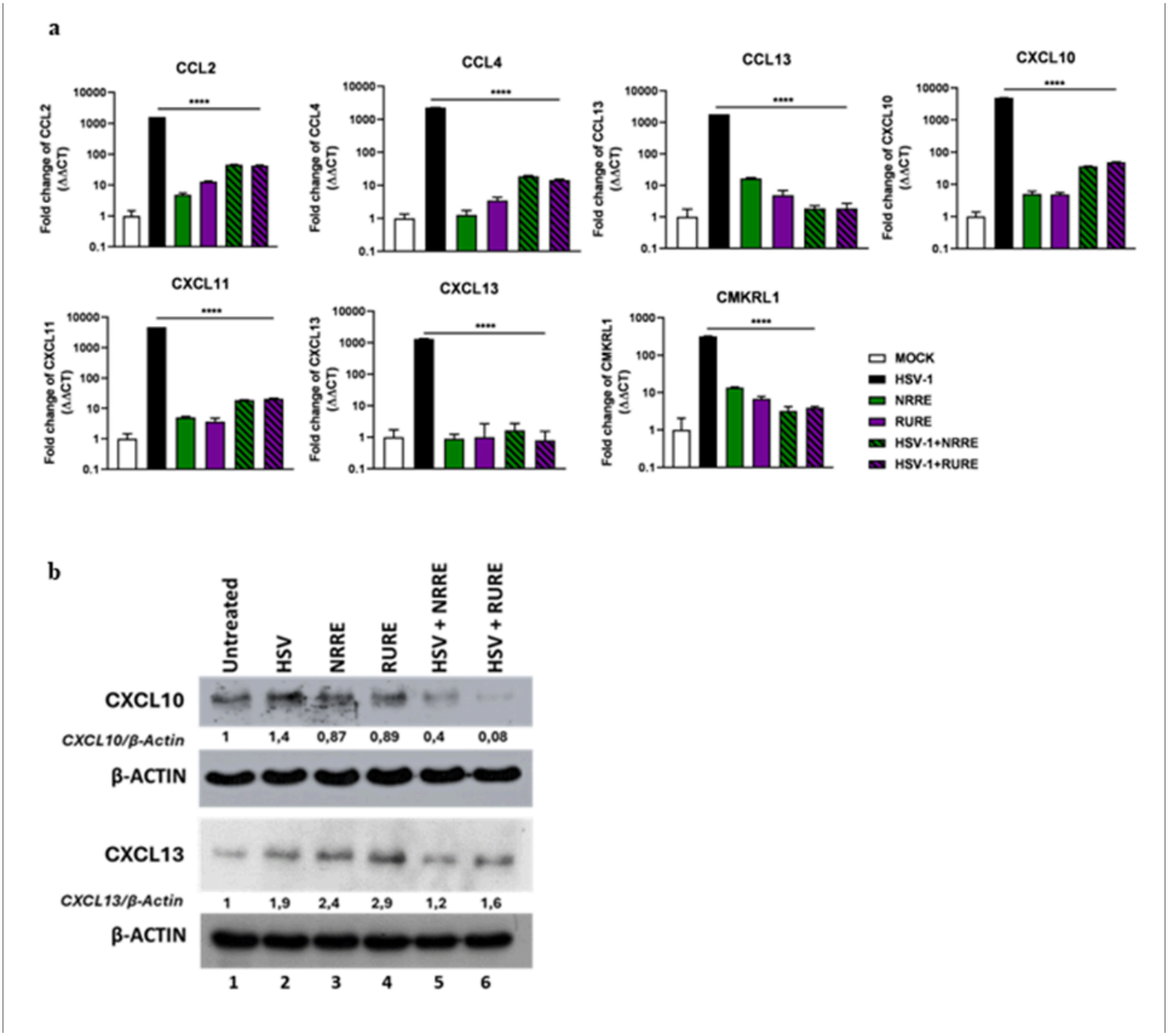

Figure 3

Validation of array data by qPCR and evaluation of CXCL10 and CXCL13 proteins following NRRE and RURE treatment in THP-1 cells. THP-1 cells were pretreated, with NRRE and RURE at 0.6 mg/mL for 1h at 37 °C and then infected with HSV-1 at 50 MOI as described in Material and Methods. One hour later, the viral inoculum was removed and replaced with growth medium containing NRRE and RURE at 0.6 mg/mL. a) Relative quantization of CCL2, CCL4, CC13, CXCL10, CXCL11, CXCL13 and CMKRL1 genes was performed using real-time quantitative PCR and analyzed by the comparative Ct method (ΔΔCt). Data are expressed as a mean (± SD) of at least three experiments. *** and **** indicates the

significance of p-values less than 0,01 and 0.001. b) Western blot analysis was performed to detect the levels of CXCL10 and CXCL13 proteins as representative cellular proteins. Densitometric analysis of CXCL10 and CXCL13 bands was normalized to β-ACTIN expression and quantified using GraphPad Prism 8 software.

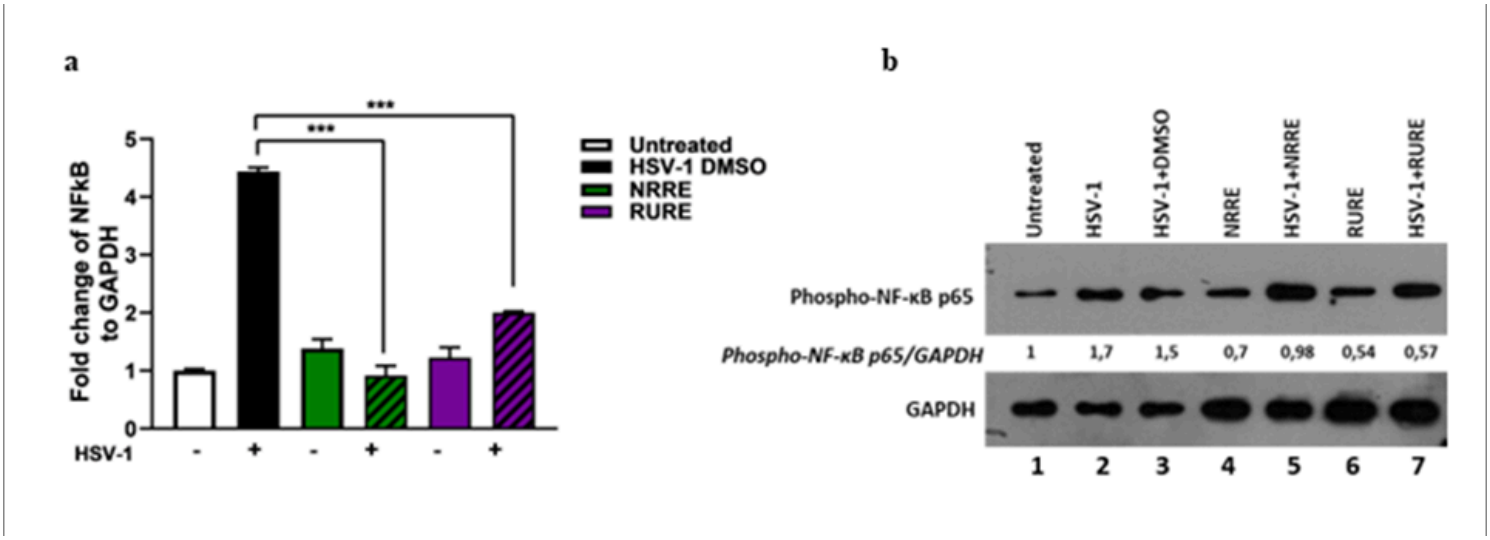

Figure 4

NF-κB activation in THP-1 infected cells. THP-1 cells were pre-treated, with NRRE and RURE at 0.6 mg/mL for 1h at 37 °C and then infected with HSV-1 at 50 MOI as described in Material and Methods. One hour later, the viral inoculum was removed and replaced with growth medium containing NRRE and RURE at 0.6 mg/mL. a) Quantitative Real-Time PCR assessed relative mRNA expression of NF-κB at 24 h p.i. b) Western blot analysis was performed to detect phospho-NF-κB p65 levels at 24h p.i. Densitometric analysis of phospho-NF-κB p65 bands was normalized to GAPDH expression and quantified using GraphPad Prism 8 software.

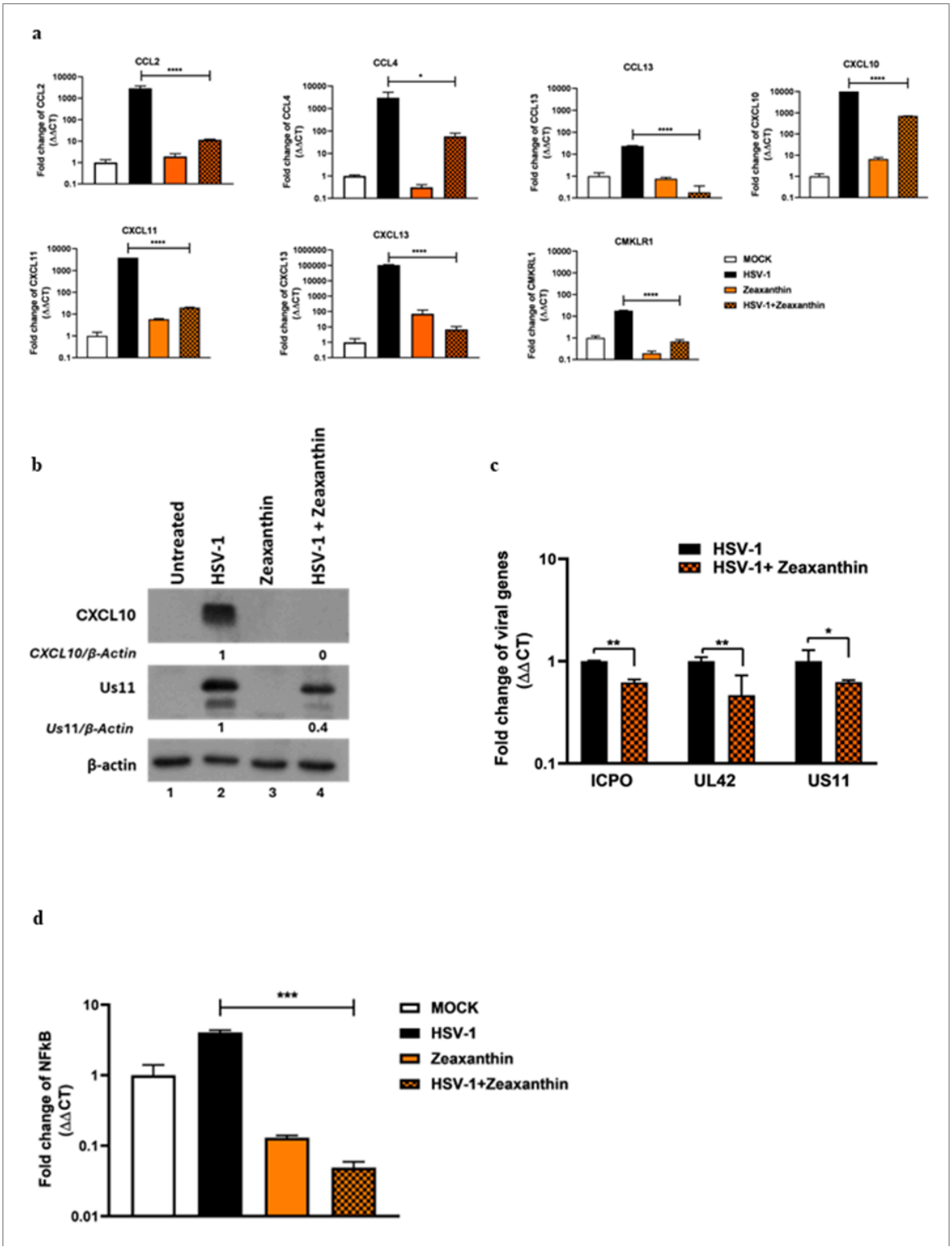

Figure 5

Inhibitory effects of zeaxanthin on HSV-1 replication, chemokines and NF-κB expression. THP-1 cells and virus were pretreated with zeaxanthin (10 μM) for 1h at 37 °C. Then, the pretreated virus was used to infect THP-1 cells at 50 MOI. 1h later, the viral inoculum was removed and replaced with growth medium in presence of zeaxanthin (10 μM). The samples were collected 24h p.i. and processed. a) Relative quantization of CCL2, CCL4, CC13, CXCL10, CXCL11, CXCL13 and CMKRL1 genes was performed using

real-time quantitative PCR and analyzed by the comparative Ct method (ΔΔCt). Data are expressed as a mean (± SD) of at least three experiments. b) western blot analysis was performed to evaluate the expression of CXCL10 and US11. The β-actin was used as a housekeeping gene. c) Real-time PCR was performed to analyze ICP0, UL42, and Us11 viral transcripts as representative genes of genetic cascade of HSV-1. d) Quantitative Real-Time PCR assessed relative mRNA levels of NF-κB at 24 h p.i. Data are expressed as a mean (± SD) of at least three experiments, and asterisks (*,**,***, ****) indicate the significance of p-values less than 0.1, 0.01, 0.001 and 0,0001, respectively.

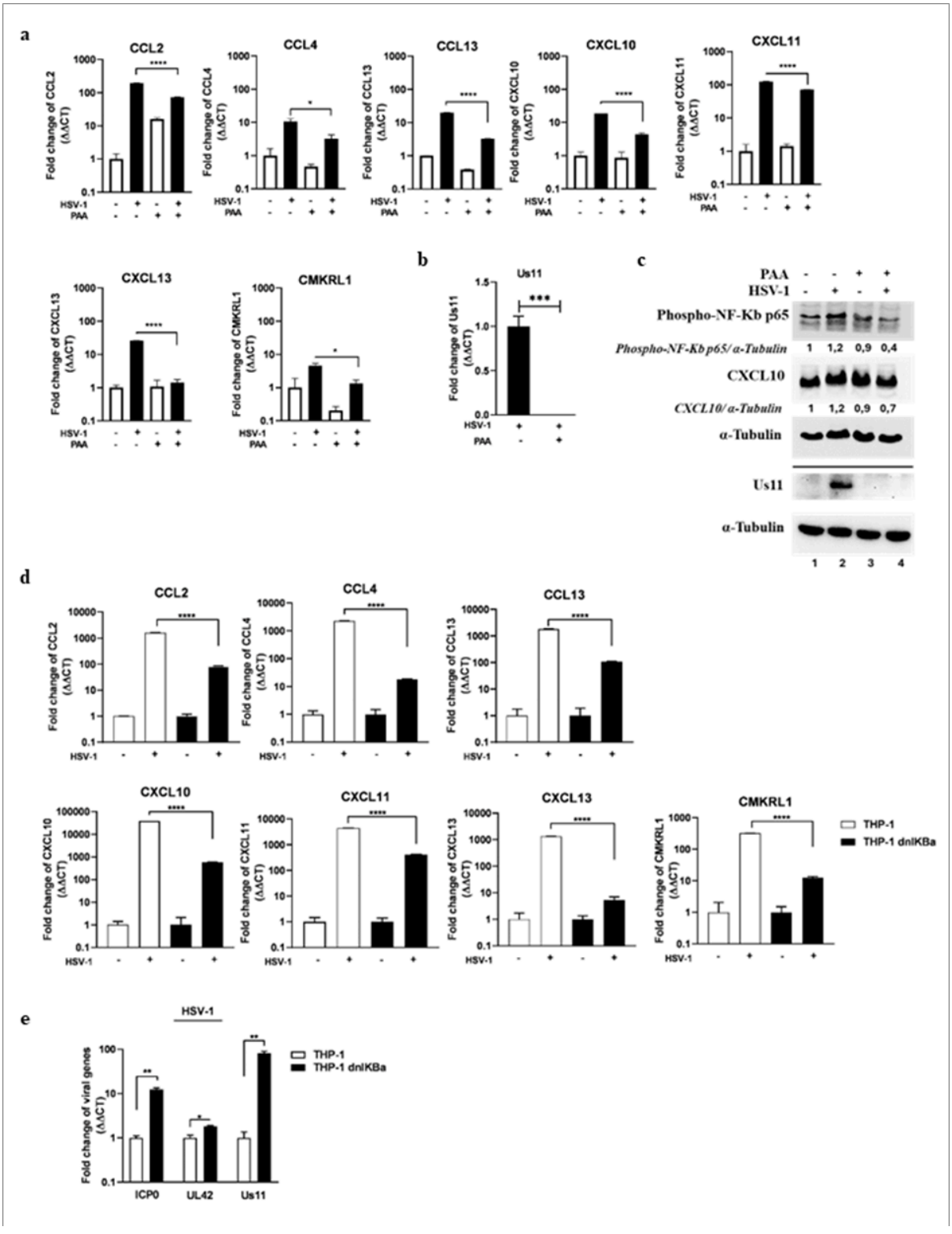

Figure 6

Comparative evaluation of chemokine transcript levels in THP-1 and THP-1 dnIκBα cell lines upon HSV-1 infection. a) THP-1 cells were infected with HSV-1 (50 MOI) in the presence or absence of phosphonoacetic acid (PAA, 300 µg/mL), an inhibitor of viral DNA replication. After 24 hours post-infection (p.i.), total RNA was extracted and analyzed by quantitative Real-Time PCR to assess the mRNA levels of CCL2, CCL4, CCL3, CXCL10, CXCL11, CXCL13, and CMKRL1. b) The efficacy of viral replication inhibition by PAA was confirmed by measuring the transcriptional levels of the viral gene Us11. c) western blot analysis was performed to analyze the expression of phospho-NF-Kb p65, CXCL10 and US11 in THP-1 cells untreated and treated with PAA. The α tubulin was used as a housekeeping gene. The grouping blots are cropped from different gels as displayed in figure with horizontal line and were captured using a ChemiDoc Touch Imaging System (Bio-Rad). d) Comparison of chemokine transcript levels in parental THP-1 and THP-1 dnIκBα cells infected with HSV-1 (50 MOI) for 24 hours. e) Transcriptional levels of viral genes (ICP0, UL42, and Us11) were measured in THP-1 and THP-1 dnIκBα cells to assess the impact of NF-κB inhibition on viral replication. Data are presented as mean ± SD from at least three independent experiments and analyzed using the ΔΔCt method.

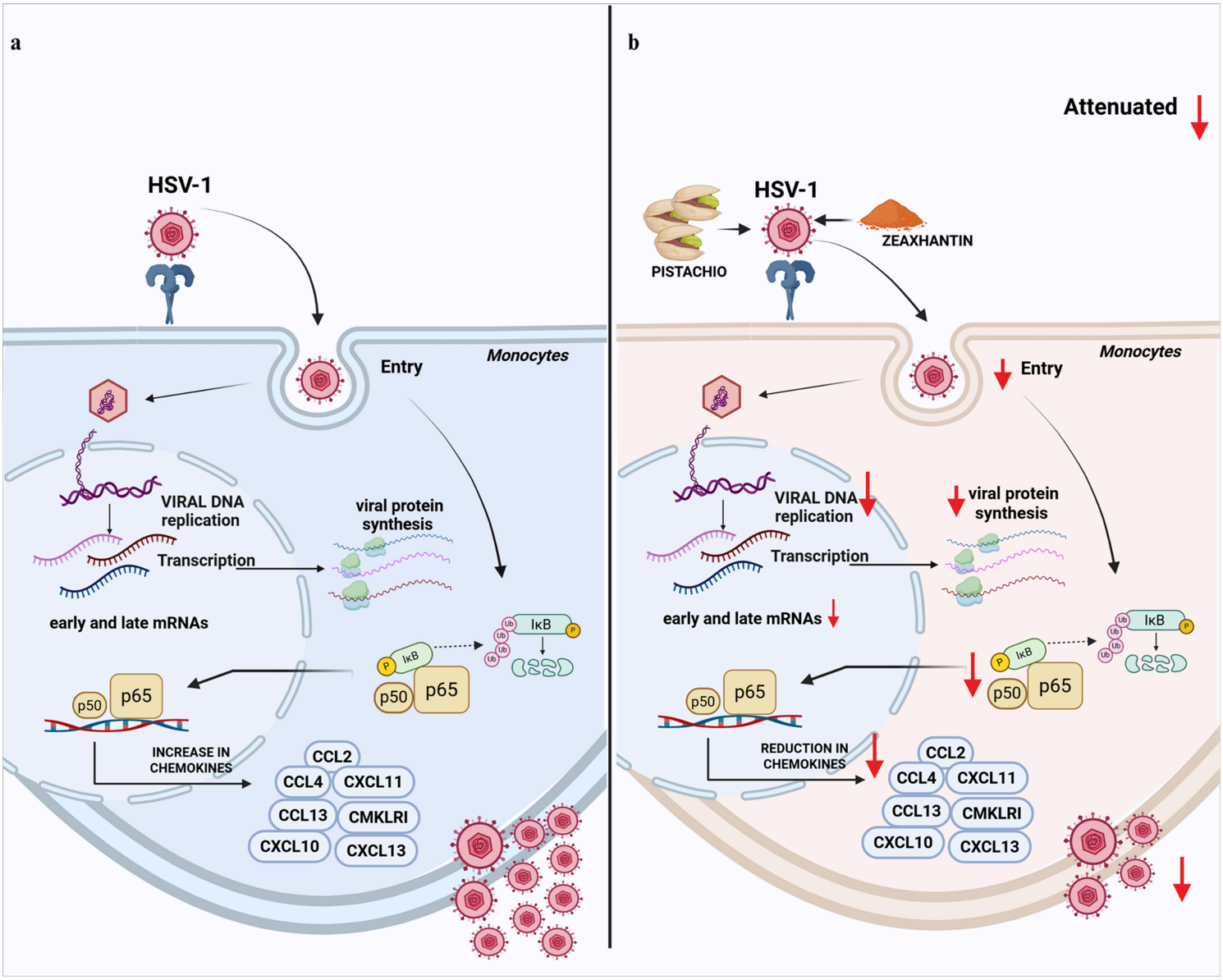

Figure 7

HSV-1-induced monocyte signaling and its modulation by pistachio extracts. a) Proposed mechanism describing the impact of HSV-1 replication on monocytes signaling, b) and its modulation by natural products. The red arrow indicates the **"**attenuation mechanism" mediated by pistachio extracts. (Created in https://BioRender.com)

Supplementary Files

This is a list of supplementary files associated with this preprint. Click to download.

- Pennisietal.2025supplementaryfile.pdf